

Experimental identification of cutting force coefficients for serrated end mills

A Kumar and M Law

Machine Tool Dynamics Laboratory, Department of Mechanical Engineering
Indian Institute of Technology Kanpur, Kanpur 208016, India

Abstract

High-performance rough machining of titanium, nickel and aluminum based alloys used in aerospace industries is often done using serrated cutters. To guide cutting process and parameter optimization for these alloys necessitates good force prediction models, which are non-trivial on account of serrations. Serrations cause the cutter radius, rake angle, helix angle, and chip thickness to continuously change along the axis of cutter. These variations can be captured using cutting force coefficients. The coefficients are often identified under orthogonal conditions and transformed using the oblique geometry of the tool. Other methods of identification assume a uniform chip thickness distribution, which does not accurately account for serrations. To avoid transformations and to overcome limitations, this paper proposes an alternate mechanistic identification method that accounts for geometric variations due to serrations by changing engagements, speeds, feeds, and axial depths of cut. Experiments are designed and a suitable response model is constructed. Model predictions are validated experimentally. Results obtained can guide cutting process optimization of these alloys using serrated cutters.

Keywords: Serrated end mills, Milling, Cutting force coefficients.

1. INTRODUCTION

Manufacturing of parts made from titanium, nickel and aluminum based alloys used in the aerospace industry often involves 80-90% of their bulk material being machined away to give parts their desired shapes. This necessitates high-productivity machining. However, parts made of these alloys are difficult-to-cut and result in large process forces. Large forces may result in parts being distorted and may also result in machining instabilities like chatter that may destroy the part, tool, and the machine. To avoid part distortions and instabilities, and to avoid machining of these super alloys with conservative cutting parameters which may reduce productivity, there is a need for tools that not only decrease process forces but also avoid machining instabilities. Serrated cutters (end mills) fit these requirements and are increasingly being used for rough machining of such difficult-to-cut materials.

Serrated cutters, unlike regular cutters, have serrations on their helical flutes and on their diameter, as shown in Figure 1. Serrated profiles may be sinusoidal, circular or trapezoidal. These serrations result in complex local geometries along the cutting edge that result in preferential reduction in cutting forces as well as an improvement against machining instabilities. To understand the influence of serrated geometries on the cutting process, modelling the geometry of these cutters for force prediction is essential to guide cutting process parameter selection for high-productivity machining. However, modelling of serrated geometry remains non-trivial, in part because of how serrations result in a continuously changing cutter radius and chip thickness along the axis of the cutter, and also in part because of how the serrated profile results in continuously changing local rake and helix angles along the cutter axis.



Figure 1 (a) Regular end mill (b) Serrated end mill

Even though the literature is replete with force models for regular end mills, there is a very limited body of published literature discussing the complexities and influence of

serrations on cutting process mechanics. Some early work on modelling serrated cutters with straight teeth was reported by Tlustý et al. [1], in which it was reported that serrated end mills reduced the workpiece-tool contact length, which in turn reduces forces and improves machining stability. Later, Campomanes [2] investigated mechanics and dynamics of serrated cutters with a sinusoidal serration profile over the helical flutes. Seminal work by Merdol and Altintas [3] and Dombovari et al. [4] described serrations on end mills using splines and investigated the reduction in cutting forces and consequent improvement in machining stability using time domain solutions.

Accurate prediction of cutting forces and machining stability for serrated cutters hinges on being able to correctly characterize the changing geometry (chip thickness and local rake and helix angle variations) of the serrated cutter along its axis. These variations can be captured using cutting force coefficients that are modelled to be a function of the serrations, as was done in [3-6]. These methods [3-6] though effective are complicated and are based on transforming the coefficients obtained from orthogonal cutting tests using the orthogonal to oblique transformation method proposed in [7]. To avoid these transformations, others [8-9] have proposed using mechanistically identified cutting force coefficients using methods that assume a uniform chip thickness distribution along the cutting edge. This assumption does not hold for serrated end mills, in which the chip thickness varies with the profile of the serrations and the engagement conditions.

To avoid using the orthogonal to oblique transformation methods used in [3-6], which require a priori an orthogonal cutting database for the workpiece material of interest which may not always be available, and to overcome the limitations of [8-9], this paper proposes an alternate mechanistic experimental identification method that accounts for how geometric variations due to serrations influence the identification of cutting force coefficients. We account for the influence of serrations by identifying coefficients by changing engagements, speeds, feeds and axial depths of cut. A response model is

motivated and developed. These identified coefficients are incorporated into the existing force models for serrated cutters [5-6] and the response model is shown to be able to reasonably predict the cutting process forces for serrated end mills.

The remainder of the paper is organized as follows: at first geometry of serrated cutters is discussed in Section 2, followed by introducing the force model for serrated cutters in Section 3. Mechanistic identification is discussed in Section 4. Section 5 motivates the response model and presents the experimental design. Experimental validation is presented in Section 6, followed by the main conclusions in Section 7.

2. GEOMETRY OF SERRATED CUTTERS

Shown in Fig. 2 is the representative geometry for sinusoidal serrations with a wavelength of 0.907mm and amplitude of 0.36mm. Along the tool axis, the waves on consecutive cutting teeth have a phase shift and because of that, cutting teeth have different instantaneous radii. Because of the geometry of serrated cutters, the rake and helix angles vary along the axis of the cutter, with the upper parts of these serrations having a lower rake angle and the lower parts having a higher rake angle. The axial immersion angle, i.e. the angle between the unit normal vector and tool edge tangent vector in x-y plane also changes continuously along the serrated profile. These geometric variations play a significant role in force prediction and are the primary mechanism responsible for a reduction in cutting forces.

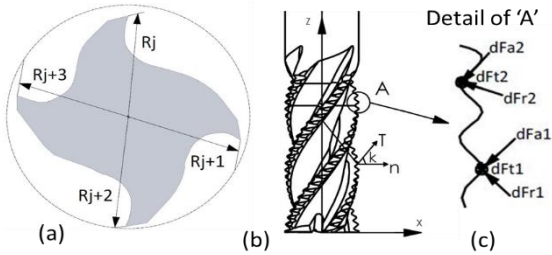


Figure 2. (a) Serrated cutter sectional view (b) end view showing surface tangent vector (T), surface normal vector (n) and axial immersion angle (\mathcal{K}), and (c) local detail showing differential milling forces and their changing directions

3. FORCE MODEL FOR SERRATED CUTTERS

Force modelling for serrated cutters is similar to the force models for regular end mills except for the directions of the differential milling forces varying along the serrations on the cutting edge, as shown in Fig. 2 (c). The linear edge model [7] is used herein for calculating the cutting forces in serrated cutters. For force calculations, milling tool is divided into small axial elements along the axis of tool. To obtain cutting forces, differential forces are calculated for each tooth at each axial element and immersion angle in one full revolution. The tangential (F_t), radial (F_r) and axial (F_a) differential forces acting on j^{th} tooth at any i^{th} axial element (dz) for immersion angle ϕ are calculated by using Eq. (1), wherein db represents the chip width [7]:

$$\begin{aligned} dF_t(i, j) &= g(\phi_{ij})[K_{te}(i, j) + K_{tc}(i, j)h(i, j)]db \\ dF_r(i, j) &= g(\phi_{ij})[K_{re}(i, j) + K_{rc}(i, j)h(i, j)]db(1) \\ dF_a(i, j) &= g(\phi_{ij})[K_{ae}(i, j) + K_{ac}(i, j)h(i, j)]db \\ db &= dz / \sin(\mathcal{K}_{ij}) \end{aligned}$$

wherein K_{tc}, K_{rc}, K_{ac} are the tangential, radial and axial cutting force coefficients and K_{te}, K_{re}, K_{ae} are the respective edge coefficients. The uncut chip thickness, h for the j^{th} tooth at axial level i for the immersion angle ϕ and local radius (R_j, R_m) for j^{th} tooth and feed rate (f_t) is calculated in Eq. (2) as [6]:

$$h(i, j) = \max \left\{ \begin{array}{l} 0 \\ \min\{R_j(z) - R_m(z) + kf_t \sin(\phi_{ij})\} \end{array} \right\} (2)$$

$$m = \begin{cases} k - j, & k - j > 0 \\ k - j + N_t, & k - j \leq 0 \end{cases}$$

where m is the successive cutting point at same axial location of z ; $k = 1, 2, \dots, N_t$; and N_t represents the number of teeth.

Differential forces in x, y, and z coordinates are calculated as follows [6]:

$$\begin{aligned} dF_x &= -dF_r \sin(\phi_j) \sin(\mathcal{K}) - dF_t \cos(\phi_j) \\ &\quad - dF_a \cos(\mathcal{K}) \sin(\phi_j) \\ dF_y &= dF_r \cos(\phi_j) \sin(\mathcal{K}) + dF_t \sin(\phi_j) \\ &\quad - dF_a \cos(\mathcal{K}) \cos(\phi_j) \end{aligned} (3)$$

$$dF_z = dF_r \cos(\mathcal{K}) - dF_a \sin(\mathcal{K})$$

Total forces in x, y and z direction are calculated by summing the differential force from all tooth and all elements:

$$F_{x,y,z}(\phi) = \sum_{z=0}^z \sum_{j=1}^{j=N_t} dF_{x,y,z}(z, j) (4)$$

Above force model is used to predict the forces in this study. Since cutting force coefficients are an input into this model, these are identified as discussed in Section 4.

4. MECHANISTIC IDENTIFICATION OF CUTTING CONSTANTS

Mechanistic modelling approach is a widely used method for identification of cutting force coefficients for cutters with complex geometries. In the mechanistic approach, a set of milling experiments are performed at different feed rates but same immersion and axial depth of cut. Experimentally measured average cutting forces ($\bar{F}_x, \bar{F}_y, \bar{F}_z$) are equated to analytical derived milling force expressions as [10]:

$$\begin{aligned} \bar{F}_x &= \left\{ \frac{N_t a c}{8\pi} [K_{tc} \cos(2\phi) - K_{rc} [2\phi - \sin(2\phi)]] \right. \\ &\quad \left. + \frac{N a}{2\pi} [-K_{te} \sin(\phi) + K_{re} \cos(\phi)] \right\}_{\phi_{st}}^{\phi_{ex}} \\ \bar{F}_y &= \left\{ \frac{N_t a c}{8\pi} [K_{rc} [2\phi - \sin(2\phi)] + [K_{tc} \cos(2\phi)]] \right. \\ &\quad \left. - \frac{N a}{2\pi} [K_{te} \cos(\phi) + K_{re} \sin(\phi)] \right\}_{\phi_{st}}^{\phi_{ex}} \\ \bar{F}_z &= \left\{ \frac{N_t a c}{8\pi} [-K_{ac} f_t \cos(\phi) + K_{ae} \phi] \right\}_{\phi_{st}}^{\phi_{ex}} \end{aligned} (5)$$

The average cutting force can be also expressed as a function of feed rate and the edge forces as follows:

$$\bar{F}_q = \bar{F}_{qc} + \bar{F}_{qe} \quad (q = x, y, z) (6)$$

Experimentally measured average cutting forces are fit using linear regression to identify the cutting components ($\bar{F}_{qc}, \bar{F}_{qe}$). In the mechanistic model, geometric properties of the cutter such as helix angle, rake angle and the relief angle, along with workpiece material, uncut chip thickness, chip width and other

variables are all embedded inside cutting coefficients. Serrations cause each of these variables to change along the axis. Hence, identification is done by designing experiments that account for these variations.

5. DESIGN OF EXPERIMENTS AND RESULTS

Design of experiments (DOE) is a statistics-based systematic method to determine the relationship between factors affecting a process and the output of that process. In the present case, the output of the process are the cutting force coefficients, and the factors affecting that process are cutting speed (A), feed rate (B), depth of cut (C), and engagement (D). Each factor has two levels, i.e. high = 1 and low = -1. A2⁴full factorial experiment is designed by varying the levels of each factor, and recording the experimental data (forces). Experiments have been conducted on a three axis vertical machining center using AL7075 workpiece and a sinusoidal serrated tool of diameter 16 mm, and four teeth. Experimental setup is shown in Figure 3.

A response model, *y* is proposed as:

$$y = intercept + k_1A + k_2B + k_3C + k_4D + k_5(AB) + k_6(AC) + k_7(BC) + k_8(AD) + k_9(BD) + k_{10}(CD) + k_{11}(ABC) + k_{12}(ABD) + k_{13}(ACD) + k_{14}(BCD) + k_{15}(ABCD) \tag{7}$$

wherein *A, B, C* and *D* are the factors, each with two levels, as described in Table 1, and *k*₁,... *k*₁₅ are coefficients to be fit to obtain a suitable response model.

Cutting forces are measured for each test, and coefficients are identified using Eq. (5-6). These coefficients are listed in Table 2 for every test. A suitable response is then obtained by fitting the *k*₁... *k*₁₅ coefficients (Eq. (7))using the ‘R’ language[11].

Six different response models are obtained that describe the three main cutting coefficients (tangential, radial, and axial) and the three edge coefficients.

The response model coefficients (*k*₁,*k*₂...*k*₁₅)for the tangential cutting force coefficient (*K*_{*t*c})are summarized using a Pareto chart in Figure 4. As is evident from Figure 4, the feed rate (factor B) and axial depth of cut (factor C) appear to be significant, as do the interactions between these factors. Large coefficients (*k*₁,*k*₂...*k*₁₅)in general suggest that those factors are more significant than others, and their relative signs gives the property effect. A positive sign indicates that with an increase in factor value there is an increase in response value, and a negative sign means a decrease in response value.

Similarly, a response model is obtained for the remainder of the five cutting force coefficients. Having obtained a response model for each of the cutting force coefficients, ability of these response models to predict forces is discussed in Section 6.

6. EXPERIMENTAL VALIDATION

The proposed mechanistic response model is validated by predicting cutting force coefficients for a cutting parameter set not used in building the response model, but for parameters that still lie within the high/low limits of the various factors. Validation is also provided by using the identified coefficients to predict the cutting forces using the force model presented in Section 3, and comparing these forces with those that are experimentally measured. Forces are predicted using CutPro [12], that has integrated inside it the model discussed in Sect. 3.

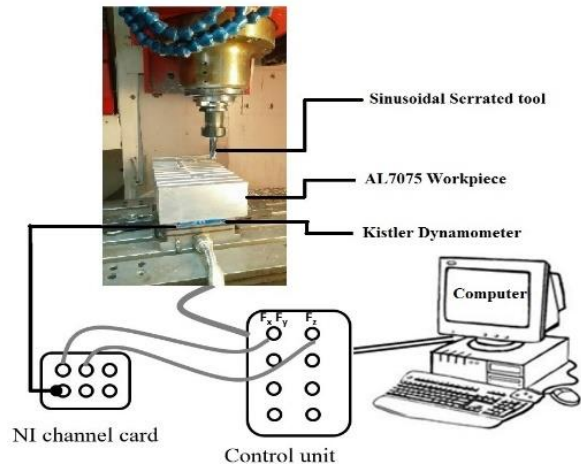


Figure 3 Experimental setup

Table 1: Factors and their levels for the experimental design

Cutting parameter	Factor	Lower limit (-)	Upper limit (+)
Spindle speed (rpm)	A	6000	8000
Feed rate (mm/tooth)	B	.05 (.05 .075 .1 .125)	.2 (.125 .175 .2)
Depth of cut (mm)	C	.68 (3/4 th of serration)	1.81 (2 full serrations)
Engagement (% of diameter)	D	50 % Engagement (Up milling)	100 % Engagement (slotting)

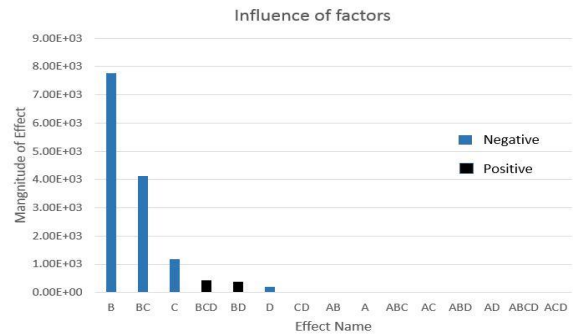


Figure 4 Pareto chart showing influence of different factors on the response model for the tangential cutting force coefficient

Representative validation for the tangential cutting force coefficient is provided in Table 3. And, as is evident the error ranges from <1% to at most ~14%, which are thought to be acceptable for serrated cutters with complex geometries.

Predicted forces are compared with measured forces in Fig. 5 for half a revolution of the cutter. Predictions are carried out at a spindle speed of 6000 RPM, an axial immersion of 0.68 mm, a feed per tooth value of 0.05 mm, and for the slotting condition. As is evident, predicted forces reasonably approximate the profile, trend and the force amplitudes.

Table 2: Identified cutting coefficients

Spindle Speed(A)	Feed Rate (B)	Depth of cut(C)	Engagement (D)	K_{tc} [N/mm ²]	K_{rc} [N/mm ²]	K_{ac} [N/mm ²]	K_{te} [N/mm]	K_{re} [N/mm]	K_{ae} [N/mm]
8000	0.05	0.68	Upmilling	1342.6	206.5	253.1	8.4	10	1.1
6000	0.2	0.68	Upmilling	1614.7	237.8	225.5	25.8	10.8	3.3
8000	0.2	0.68	Upmilling	1328.9	370.7	209	9	7	3.1
6000	0.05	1.81	Upmilling	1143.2	125.4	163	5.4	1.5	0.1
8000	0.05	1.81	Upmilling	885.4	120.6	136.6	8.3	4.3	0.1
6000	0.05	0.68	Upmilling	1814.8	450.2	276	12	1.4	2.2
6000	0.2	1.81	Upmilling	880.1	123.2	66.1	23.6	3.6	6.9
8000	0.2	1.81	Upmilling	824.5	172.4	35.2	11.2	1.2	7.7
6000	0.05	0.68	Slotting	1334.5	503.3	182.3	7.6	12.3	0.04
8000	0.05	0.68	Slotting	1174.7	423.8	208.9	4.6	13.9	0.6
6000	0.2	0.68	Slotting	1240	428.1	191.2	15.9	20.3	1.2
8000	0.2	0.68	Slotting	1026.5	392.6	126.4	21.3	15.1	6.2
6000	0.05	1.81	Slotting	705.7	233.6	115.4	10.3	11.1	0.3
8000	0.05	1.81	Slotting	691.5	173.6	86.6	7.4	11.6	0.8
6000	0.2	1.81	Slotting	925.6	266.7	61	12.3	7.9	3.8
8000	0.2	1.81	Slotting	803.5	218	23.7	2.8	8.3	5.7

Table 3: Experimental validation of tangential cutting force coefficient (K_{tc} [N/mm²])

Factors				Predicted using response model	Identified experimentally	Error (%)
A	B	C	D			
6000	.05	.68	50%	1334.23	1334.5	0.02
7000	0.2	1	50%	1056.6	1008.5	4.78
7000	0.2	1.2	100%	1186	1033.5	14
8000	0.2	0.8	50%	1002.2	995.248	7.1

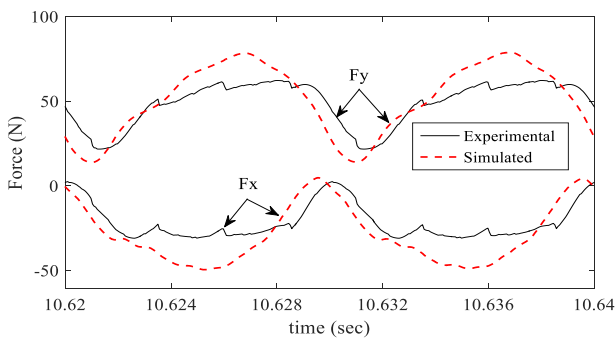


Fig.5 Measured and predicted forces in the X and Y directions.

7. CONCLUSIONS

Cutting force calculations involves identification of cutting force coefficients that are influenced by the serrated geometry of the cutter. Since the serrated geometry such as cutter radius, rake angle, helix angle, and chip thickness change continuously along the axis of cutter, the classical mechanistic calibration of these coefficients cannot be employed on serrated cutters. Hence, this paper presented an alternate mechanistic response model that accounts for geometric variations due to serrations by changing engagements, speeds, feeds, and axial depths of cut. The proposed mechanistic response model is validated by predicting cutting force coefficients for a cutting parameter set not used in building the response model, and predicted cutting force coefficient shows error ranges from <1% to at most ~14%, which are thought to be acceptable for serrated cutters with complex geometries. Experimentally identified cutting force coefficients used in predicting forces reasonably

approximate the profile, trend and amplitudes of measured forces. Results obtained can guide cutting process optimization of difficult-to-cut-materials using serrated cutters.

References

- [1] J. Tlustý, F. Ismail and W. Zaton. Use of Special Milling Cutters against Chatter, NAMRC 11, University of Wisconsin, SME, pp. 408-415, 1983
- [2] M.L. Campomanes. Kinematics and Dynamics of Milling with Roughing Endmills. Metal Cutting and High Speed Machining, Kluwer Academic/Plenum Publishers, 2002.
- [3] S.D. Merdol, Y. Altintas, Mechanics and dynamics of serrated cylindrical and tapered end mills, Journal of Manufacturing Science and Engineering, Vol. 126 (2), pp.317–326, 2004.
- [4] Z. Dombovari, Y. Altintas and G. Stepan. The effect of serration on mechanics and stability of milling cutters, International Journal of Machine Tools and Manufacture, Vol. 50 (6), pp. 511-520, 2010.
- [5] R. Koca and E. Budak. Optimization of Serrated End Mills for Reduced Cutting Energy & Higher Stability, Procedia CIRP, 8, pp. 570-575, 2013.
- [6] F. Tehranizadeh and E. Budak. Design of Serrated End Mills for Improved Productivity, Procedia CIRP, 58, 2017.
- [7] E. Budak, Y. Altintas, and E. J. A. Armarego. Prediction of Milling Force Coefficients from orthogonal Cutting Data. Transactions of the ASME Journal of Engineering Industry, Vol. 118, pp.216-223, 1996.
- [8] A. Hosseini, B.M. Imani and H.A. Kishawy. Mechanistic modelling for cutting with serrated end mills—a parametric representation approach. Journal of Engineering Manufacture, Vol. 225, pp.1019 – 1032, 2011.
- [9] B.M. Imani, H. El-Mounayri and S.A. Hosseini. Analytical Chip Load Prediction for Rough End Mills. TICME2007, pp.10–13, 2007, Tehran, Iran.
- [10] Y. Altintas, Manufacturing Automation, Cambridge University Press, 2000
- [11] R language, Austria. URL: <http://www.Rproject.org/>
- [12] CutPro simulation software, MAL, UBC-Canada. URL: <https://www.malinc.com/products/cutpro>